Supporting Information

Isaacson et al. 10.1073/pnas.1018821108

SI Materials and Methods

1 Equivalent Variable Diffusion Constant Model to [1]. Let $p(\boldsymbol{x},t) = \rho(\boldsymbol{x},t)\exp(-U(\boldsymbol{x})/k_{\mathrm{B}}T)$. With this choice [**1**] becomes

$$e^{-U(\boldsymbol{x})/k_{\mathrm{B}}T}\frac{\partial \rho}{\partial t} = \nabla\cdot(De^{-U(\boldsymbol{x})/k_{\mathrm{B}}T}\nabla\rho).$$

We may interpret this equation as describing the diffusion of a particle with variable diffusion constant, $D\exp(-U(\boldsymbol{x})/k_{\mathrm{B}}T)$, in the presence of a "diffusive capacity," $\exp(-U(\boldsymbol{x})/k_{\mathrm{B}}T)$. Here $\rho(\boldsymbol{x},t)$ represents the probability per unit *available* volume, with the diffusion capacity representing the available volume fraction (i.e., the available volume per unit volume).

2 Numerical Discretization of the Fokker–Plank Equation. In this section we show how to derive the discretization of the Fokker–Planck [**1**] in the *Mathematical Model* section of the main text with coefficients given by [**5**].

We begin by considering the one-dimensional version of [**1**] that we rewrite as

$$\frac{\partial p}{\partial t}(x,t) + \frac{\partial F}{\partial x}(x,t) = 0, \qquad \textbf{[S1]}$$

where the flux, $F(x,t)$ is given by

$$F(x,t) = -D\left(\frac{\partial p}{\partial x}(x,t) + \frac{p(x,t)}{k_{\mathrm{B}}T}\frac{\partial U}{\partial x}(\boldsymbol{x})\right). \qquad \textbf{[S2]}$$

Our discretization procedure is similar to that of (1), though as we shall show we obtain different discretization coefficients. Let $p_i(t) \approx p(ih,t)$ for h a specified mesh width, and define U_i and F_i similarly. At nonboundary points we assume a discretization of the form

$$\frac{dp_i}{dt}(t) + \frac{1}{h}(F_{i+1/2} - F_{i-1/2}) = 0, \qquad \textbf{[S3]}$$

where

$$F_{i+1/2} = \alpha(U_{i+1}-U_i)p_i - \beta(U_{i+1}-U_i)p_{i+1}. \qquad \textbf{[S4]}$$

Here $\alpha(\cdot)$ and $\beta(\cdot)$ are functions to be determined. We may rewrite this expression as

$$F_{i+1/2} = [\alpha(U_{i+1}-U_i) - \beta(U_{i+1}-U_i)]\left(\frac{p_i+p_{i+1}}{2}\right) + [\alpha(U_{i+1}-U_i) + \beta(U_{i+1}-U_i)]\left(\frac{p_i-p_{i+1}}{2}\right). \qquad \textbf{[S5]}$$

For the diffusive portion of the Fokker–Plank [**S1**] we would like to recover the standard second-order discretization of the Laplacian on $\mathbb{R}$,

$$\frac{\partial^2 p}{\partial x^2}(ih,t) \approx \frac{1}{h^2}(p_{i+1} + p_{i-1} - 2p_i). \qquad \textbf{[S6]}$$

We therefore impose that

$$\alpha(U_{i+1}-U_i) + \beta(U_{i+1}-U_i) = \frac{2D}{h}. \qquad \textbf{[S7]}$$

With this choice, the second term in [**S5**] then reduces to the standard discretization of the diffusive flux, giving rise to the discrete Laplacian [**S6**] in [**S3**]. It remains to choose α and β so that the first term in [**S5**] represents a discretization of the flux arising from drift induced by the potential $U(x)$.

Let $p_i^{\mathrm{eq}} = \lim_{t\to\infty} p_i(t)$ denote the steady state value of $p_i(t)$, and $p^{\mathrm{eq}}(x)$ the steady state value of $p(x,t)$. We assume that the steady state probability the molecule is in voxel i is $p_i^{\mathrm{eq}}h$. As in ref. 1, at thermodynamic equilibrium we expect the probability density the molecule is at position x to be proportional to the Boltzmann distribution

$$p^{\mathrm{eq}}(x) \propto e^{-U(x)/k_{\mathrm{B}}T}.$$

We therefore require that

$$p_{i+1}^{\mathrm{eq}} = p_i^{\mathrm{eq}} e^{(U_i-U_{i+1})/k_{\mathrm{B}}T}.$$

Moreover, at thermodynamic equilibrium detailed balance requires that the probability flux between neighboring voxels should balance, that is

$$F_{i+1/2} = 0.$$

Combining the last two equations we find that

$$\alpha(U_{i+1}-U_i)e^{(U_{i+1}-U_i)/k_{\mathrm{B}}T} = \beta(U_{i+1}-U_i). \qquad \textbf{[S8]}$$

Solving Eqs. [**S7**] and [**S8**] for the functions α and β, we obtain that

$$\alpha(U_{i+1}-U_i) = \frac{2D}{h}\frac{1}{e^{(U_{i+1}-U_i)/k_{\mathrm{B}}T}+1},$$
$$\beta(U_{i+1}-U_i) = \frac{2D}{h}\frac{1}{e^{(U_i-U_{i+1})/k_{\mathrm{B}}T}+1}.$$

By Taylor Series expanding the truncation error associated with the discretization it can be seen that these expressions give a second-order discretization in h. (Here we have ignored the issue of discretizing boundary conditions.) The coefficients of p_i, p_{i+1}, and p_{i-1} in [**S3**] determined by α and β then give the jump rates [**6**] for voxels that are uncut by the nuclear membrane.

In three-dimensions, for voxels that are cut by the nuclear membrane we follow the approach of ref. 2. The three-dimensional equivalents of the flux [**S4**] are used in the finite-volume embedded boundary method derived in ref. 2 to give the jump rates [**5**].

3 Average Time to Locate a Target in One, Two, and Three Dimensions. Consider the problem of finding a point, circular, or spherical target in one, two, or three dimensions. Assume that binding occurs immediately upon reaching the target's boundary and that, for simplicity, the domain in which the search takes place is a concentric point, circle, or sphere to the target. If the target has radius r_{b} and the outer boundary has radius r_{o}, the probability density for the diffusing particle to be at position $\boldsymbol{x}$ at time t satisfies [**1**] with $U(\boldsymbol{x}) = 0$ and $\boldsymbol{x}_{\mathrm{b}} = 0$ (in the domain, $\Omega = \{\boldsymbol{x} | r_{\mathrm{b}} < |\boldsymbol{x}| < r_{\mathrm{o}}\}\perp$). In addition, the boundary conditions remain [**2**] and [**3**]. If we assume the initial position of the particle is uniformly distributed on the sphere (or circle or point), $|\boldsymbol{x}| = r$, the solution to [**1**] is radially symmetric.

Denote by $T_d(r)$ the average exit time for the particle to locate and bind to the target in d dimensions, given that the initial position of the particle is $|\boldsymbol{x}| = r$. Then (see ref. 3),

$$\frac{1}{r^{d-1}}\frac{d}{dr}\left(r^{d-1}\frac{dT_d}{dr}\right) = -\frac{1}{D},$$

with the boundary conditions that

$$T_d(r_b) = 0, \qquad \frac{dT_d}{dr}(r_o) = 0.$$

Solving these equations, we find that

$$T_d(r) = \frac{r_b^2 - r^2}{2dD} + \frac{r_o^d}{dD}(f_d(r) - f_d(r_b)),$$

where

$$f_d(r) = \begin{cases} r, & d = 1, \\ \ln(r), & d = 2, \\ \frac{-1}{r}, & d = 3. \end{cases}$$

By examining derivatives, it can be seen that $T_1(r) < T_2(r) < T_3(r)$ for $r_b < r \leq r_o$. Moreover, if we assume that the particle begins its search at $r = r_o$, and that the target radius is substantially smaller than the domain radius ($r_o \gg r_b$), we see that

$$T_d(r_o) \sim \begin{cases} \frac{r_o^2}{2D}, & d = 1, \\ \frac{r_o^2 \ln(r_o)}{2D}, & d = 2, \\ \frac{r_o^3}{3r_bD}, & d = 3, \end{cases}$$

as $r_o \to \infty$. These scalings demonstrate that in a large domain it will take significantly longer to find the (small) target as the dimension is increased (particularly in three-dimensions).

1. Wang H, Peskin CS, Elston TC (2003) A robust numerical algorithm for studying biomolecular transport processes. *J Theor Biol* 221:491–511.
2. Isaacson SA, Peskin CS (2006) Incorporating diffusion in complex geometries into stochastic chemical kinetics simulations. *SIAM J Sci Comput* 28:47–74.
3. Gardiner CW (1996) *Handbook of Stochastic Methods for Physics, Chemistry, and the Natural Sciences, Springer Series in Synergetics* (Springer, New York) Vol. 13, 2nd edition.

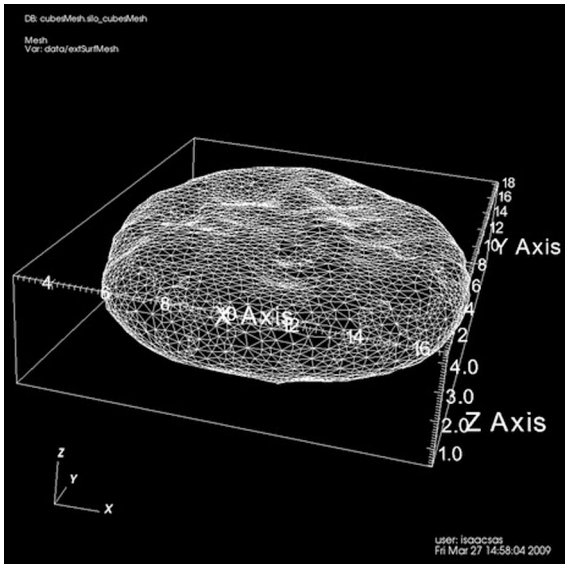

Movie S1. Shows the triangulated nuclear membrane surface reconstructed from the nuclear pore fluorescence data of ref. 1. Spatial units are in micrometers.

1 Schermelleh L, et al. (2008) Subdiffraction multicolor imaging of the nuclear periphery with 3D structure illumination microscopy. *Science* 320:1332–1336.

Movie S1 (MOV)

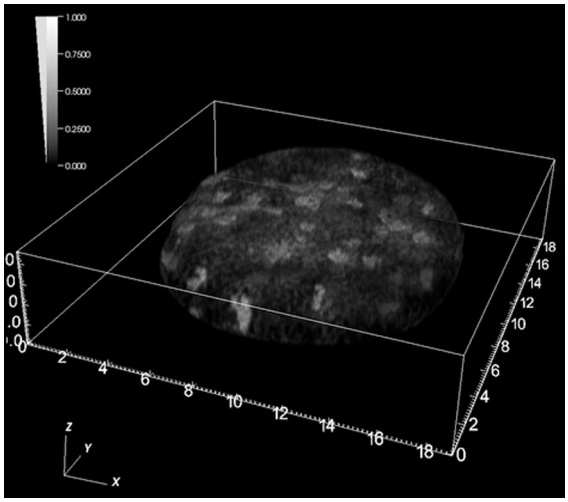

Movie S2. Shows a rotating volume rendering of the normalized DNA fluorescence intensity field, I_i. Note, the rendering is attenuated to allow the viewer to see within the cell. As such, the field appears "clumpier" than it actually is. Spatial units are in micrometers.
Movie S2 (MOV)

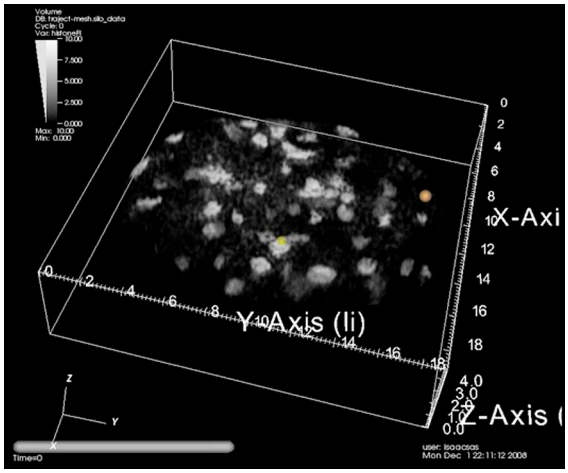

Movie S3. Shows a typical trajectory of the protein searching for the binding site. Spatial units are in micrometers, and time is in seconds. The diffusion constant of the protein was chosen to be $1\ \mu\mathrm{m}^2/\mathrm{s}$. Due to the large number of spatial jumps between voxels, the position of the protein is only shown every .01 s after an initial jump of 1729.14 s. Note, the yellow sphere corresponds to the position of the binding site, whereas the brown sphere corresponds to the diffusing protein. The size of the spheres was chosen solely for visualization purposes, and the volume rendering of the potential field was attenuated so that the viewer could see into the volume. $\tilde{U} = 10k_{\mathrm{B}}T$ in the simulation.
Movie S3 (MOV)